Statistical Comparison of Map Projection Distortions Within Irregular Areas

A. Jon Kimerling, W. Scott Overton, and Denis White

ABSTRACT. We describe a statistical sampling approach to characterizing and comparing map projection distortion within irregular areas. Statistical measures of distortion, coupled with traditional distortion isoline maps, give a clear picture of map projection distortion for irregularly shaped areas, like the United States or portions of it. We calculate cumulative distribution functions and several descriptive statistics from the distortion measures. In our example, we compare two common projections, the Lambert azimuthal equal area and the Albers conic equal area, over the conterminous United States and over two subregions. In addition to scale and angle distortion, we develop a new measure of shape distortion. Our analyses show that the Lambert projection has lower mean and median shape distortion when compared over the conterminous U.S., whereas the Albers projection has a lower maximum distortion and distortion variance for all three distortion measures. The cumulative distribution functions are substantially different and show that the Lambert projection has lower distortion values for approximately 80% of the sample points. We also compare a large unrestricted random sample with a systematic random sample. The sample size is large enough that the unrestricted and systematic samples give virtually identical results.

KEYWORDS: map projection distortion, statistical sampling, Monte Carlo integration

Cartographers often must select the optimal map projection for large irregular areas, such as nations or continents, based upon specific design criteria that relate to map projection distortion. In a recent example, White et al. (1992) selected a map projection for the truncated icosahedron global surface tessellation that forms the geometrical framework for an environmental monitoring program. The monitoring program required an equal area map projection surface for the 20 spherical hexagons and 12 spherical pentagons comprising the tessellation, upon each of which a regular sampling grid could be positioned randomly. The sampling criteria dictated the selection of an equal-area map projection for the hexagon and pentagon faces, with the provision that map projection distortion not be excessive within the portion of the hexagon containing the conterminous United States.

Young's Rule (as described in Maling 1973, 165) guides the selection of the equal area projection for the regular spherical hexagons and pentagons of the truncated icosahedron tessellation. The rule is that an area of the earth approximately circular in outline is best represented by one of the azimuthal projections, whereas asymmetrical or elongated areas are better mapped using conic or cylindrical projections. By this rule, the Lambert projection would be chosen for the truncated icosahedron hexagon and pentagon faces. (When placing a grid across adjacent faces, however, the recent projection developed by Snyder 1992 may be preferable). But is this projection adequate for the 48 continental United States that fit into one hexagon? To answer this question, and to address the more general question of comparing the distortion characteristics of different projections for an irregular portion of the earth, we must consider how to compute and compare distortion measures for irregularly shaped areas.

A. Jon Kimerling is Professor of Geography in the Department of Geosciences, **W. Scott Overton** is Emeritus Professor of Statistics in the Department of Statistics, and **Denis White** is a research geographer with the Department of Geosciences, Oregon State University, Wilkinson Hall 104, Corvallis, OR 97331-5506.

Previous Map Distortion Assessment Methods

One method for assessing map projection distortion is to graphically display the surface formed by the values of scale factors or other distortion measures (see Robinson et al. 1995, 68-89 for examples). These well-known, basic distortion measures are briefly described in Appendix 1.

Isoline maps of these measures allow one to easily see the spatial pattern of distortion across the area as well as the position of the point or line(s) of zero distortion, but they do not necessarily give a good picture of the average distortion or the distortion extremes within an irregular area.

A second method comes from the mathematical theory of minimum-error map projections. The basic idea, developed by Airy and Clarke in the nineteenth century, is that "the sums of squares of scale errors integrated throughout the area of the map should have minimum value" (Maling 1973, 172). An alternative statement of this criterion is that the average squared scale error for the selected projection should be less than the average for any alternative projection. This is, of course, an application of the method of least squares described by Gauss in 1795. One could also require that the average squared scale error over a specific part of the surface area be minimized. For areas bounded by parallels, this requirement could be studied by using Maling's graphs (1973, 169-71), plotting magnitudes of distortion measures against angular distance from the point or line(s) of tangency for various projections. However, a more complex numerical integration method is required when analyzing irregular areas such as the conterminous United States.

The best-known attempts at using numerical integration methods to assess and minimize average scale distortion are found in the work of Tsinger in 1916 and Kavrayskiy in 1934 (Snyder 1987, 99). Their efforts were directed toward selecting optimal standard parallels for the Albers equal area conic projection. They found standard parallels that minimized scale distortions for the land area being mapped, accomplishing this by weighting narrow latitude bands according to the amount of land area contained in each. This approach works well for the Albers and other projections, where lines of equal distortion follow parallels.

A simple modification provides an equivalent analysis for the Lambert projection. Since distortion is equal at all points equidistant from the projection center, numerical integration is accomplished by weighting each radial band by the land area contained. This illustrates the problem-specific structure that is required by numerical integration. The two projections being compared require different structures.

Robinson (1951) extended earlier work by Behrmann in which isolines of maximum angular deformation were used to delineate polygons of "constant" distortion. The areas of these polygons were measured by planimeter and used to compute mean values. Robinson applied this technique to arbitrary areas of interest—in his case a generalized representation of land masses over the earth—by computing the land areas for 5° latitude bands and then calculating maximum angular and area distortion values for different projections in these bands. The maximum values were then averaged as in the procedure used by Behrmann.

More recently, Dyer and Snyder (1989) used a small set of points arrayed on a 2° graticule over an area of interest to compute a minimum-error equal area projection. They minimized the distortion of the Tissot Indicatrix using iterated least squares analysis on equal area preserving transformations of plane coordinates of an initial equal area projection. Snyder (1994) describes experiments using the least squares criterion on graticule cells weighted by surface area on the sphere.

Monte Carlo integration (Hammersly and Handscomb 1964) also can provide this assessment. Unlike the methods of Dyer and Snyder, Monte Carlo integration does not have to be tailored to the method of projection, which makes comparisons easier. Tobler (1964) first proposed random simulation of distortion properties. This was partly in response to the newly developed digital computer, which made it possible to compute angular and areal distortion from a statistically valid number of randomly placed spherical and plane triangles. The method was not rigorously evaluated from the statistical viewpoint, however, and the rest of this paper is devoted to demonstrating that statistical simulation of numerical integration provides similar analyses without tedious attention to the patterns of distortion or to regional boundaries. Monte Carlo integration will be demonstrated for the conterminous United States using the Lambert azimuthal equal area projection and the Albers conic equal area projection. We choose the Lambert projection because of its suitability for a hexagonal area of interest and want to compare it to the commonly used Albers projection on irregular subsets of that area.

Statistical Analysis of Map Projection Distortion

Although the use of statistical sampling in map projection distortion analysis may seem novel, sampling methods for the estimation of areas of irregular map regions associated with ranges of surface values such as elevation are well known

(Muehrcke 1986; Maling 1989). The dot planimeter is perhaps the best-known sampling device for this purpose. A regular or (systematic) random array of dots on clear film is placed over the irregular map area and the dots falling within the area are tallied and multiplied by the unit area value of a dot in order to estimate the total surface area. If the elevation or any other value at each point can be determined, the average surface height or volume can be estimated easily. The average scale distortion for the portion of a truncated icosahedron hexagonal face containing the conterminous United States could be determined with a dot planimeter, but the determination of distortion at each point would be tedious. A digitally created dot array is superior, allowing determination of distortion from the explicit point location.

Dot planimeters compute surface area by simulation of numerical integration of finite areas through systematic or random sampling. As with any sampling effort, the design features to be determined prior to application include the geometrical arrangement of sample points, the number or density of points, the nature or specification of the surface to be analyzed, and the descriptive parameters that will be used to characterize the surface.

Numerical Integration and the Statistical Perspective

Systematic grids with points arranged as vertices of squares are commonly used in numerical integration. More complex patterns of points are sometimes used for higher order surfaces. A common example is provided by the Newton-Cotes formulas for polynomials (Press et al. 1988). For any complex region or surface, the patterns and formulas can be kept more simple if the number of sample points is increased. A particular sampling pattern and numerical integration formula may give exact integrals for certain surfaces, but inexact integrals for higher order surfaces. Irregular regions pose another source of error due to the irregular boundary effects. We focus here on regular grids of high density applied to irregular regions in two dimensions; the edge-effect error is reduced by density, but is not easily eliminated.

The statistical perspective provides another way of treating this error. We introduce a random sampling element into the process, providing a different set of sample points for each realization of the "numerical integration" process. As a consequence, the error also varies among realizations, and statistical assessment of precision then follows the familiar statements of bias, variance, and confidence bounds. If the average error over all realizations is zero, then bias is zero, and the average squared error of an unbiased estimator is its variance. Appropriately applied randomization has the capacity for eliminating the bias, or reducing it to a negligible level, regardless of the order of the surface, and standards of precision can be met by appropriate choice of sample size.

The simplest sampling design is an unrestricted random sample (URS) of points; when used for integration, this design historically has been referred to as Monte Carlo integration (Hammersly and Handscomb 1964; Press et al. 1988). The properties of such a sample are provided by the theory of independent random variables, which is the basis for much of statistics (refer to any elementary text in mathematical statistics or methods such as that presented in, for example, Snedecor and Cochran 1980). The random variable is the value of the response at a randomly located point. Two independent random points give two independent values of the random variable, and so on. The expected value of this random variable is the mean value of the response over the region, as determined by exact integration, so that the mean of the sample of response values is an unbiased estimator of the true mean, and, by implication, the sample analysis is a form of numerical integration.

It is in the representation of the cumulative distribution function (CDF) of the random variable that the URS most satisfyingly fulfills the concept of Monte Carlo integration. Designate the region of the United States in which the distortion measure is equal to or less than a particular value. Then the number of sample points that fall in this region provides a Monte Carlo estimate of the area of the region, but without delineating it. The empirical CDF is the representation of this estimated integral for all observed values of the distortion measure, scaled by the total area of the United States, itself estimated by the total number of points falling in the United States. The empirical CDF is the comprehensive statistic summarizing the data.

A systematic sample behaves similarly (Moran 1950). This form, with regularly spaced and equally weighted observations, is favored for simple numerical integration designs when sample size is not limiting, but requires special treatment at the edges of the region of integration (see, for example, Yates 1949). Random placement of the grid of points effectively simulates these edge adjustments, with the result that the systematic

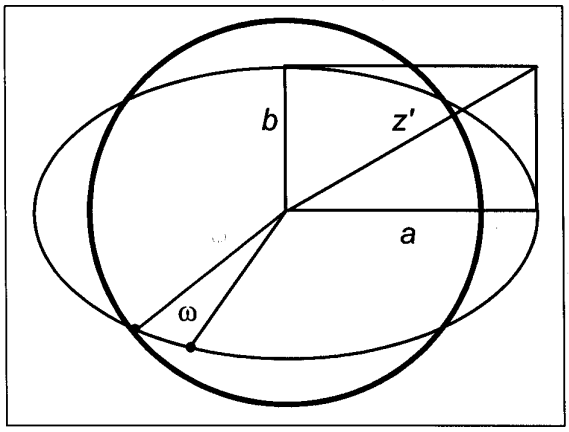

Distortion Parameters on Tissot's Indicatrix

Figure 1. The geometric relationships between distortion parameters of interest displayed on a Tissot Indicatrix for a projection in normal aspect.

mean is nearly unbiased for the true mean as determined by exact integration; this bias diminishes as the grid density increases. The theory of systematic sampling comes from a subset of statistical theory called sampling theory. It is generally recognized that systematic sampling is more precise for a given sample size than unrestricted random sampling when the surface is well behaved, as in the current application. However, it is sometimes difficult to document the gain in precision from analysis of a sample. Systematic sampling with a square grid is a common design; a triangular grid will give slightly greater precision (Matérn 1986).

Sample size is an important consideration in field sampling, but it is not an issue in the present application because little additional cost is incurred even by doubling the sample size. We want a sample size such that a major increase will produce an unimportant change in the results. That is, the sample size we will use for Monte Carlo analysis will be sufficiently large that we can consider the results as having been obtained by integration. Note too that sample size flexibility of the URS over a regular systematic grid is an additional advantage in the present context. The regular triangular grid can expand by no less than a factor of three if the randomization is performed at the original density (White et al. 1992). On the other hand, the URS can be expanded by the addition of another independent URS of whatever size.

The systematic sampling grid for the conterminous United States described in White et al. (1992) will be used to illustrate the application of a systematic sample to the assessment of map projection distortion. This sampling density was chosen for specific purposes, but we use it as an example in order to compare the results at this density to those obtained from Monte Carlo integration. We also apply this assessment method to portions of the United States; small subregions will have smaller samples, and the precision of characterization of distortion may become a factor when addressing smaller areas.

Distortion Measures

The distortion measures selected to characterize a map projection should be well suited to describing patterns of distortion for a single projection, as well as for comparing distortion on several projections. We are interested, here, in equal area projections, therefore we need measures that indicate scale distortion, angular deformation, and total shape distortion at a point. For scale distortion we may use a or b (or h or k), and for angular distortion ω (see Appendix 1). But we are also interested in a measure of total shape distortion that combines the distortion in the two orthogonal directions represented by a and b (or h and k). For this shape distortion, two possibilities are $[(1-a)^2 + (1-b)^2]$ or $[(1-h)^2 + (1-k)^2]$, both fundamental quantities used in the formulation of minimum error map projections (Maling 1973). More desirable is a normalized measure, having a value of 0.0 at the point of tangency or along the line or lines of tangency (standard parallels), and values greater than 0.0 elsewhere. The measure

$$\sqrt{a^2+b^2} - \sqrt{2},$$

the normalized magnitude of a vector formed by the lengths of the orthogonal a and b axes in the Tissot Indicatrix, has this property for equal area projections. In this paper we use

$$z = \sqrt{h^2+k^2} - \sqrt{2}$$

as the distortion measure and call it the "shape" distortion. We use h and k rather than a and b since $\theta' = 90°$ for normal aspect azimuthal, conic, and cylindrical equal area projections, so that $a = k$ or $a = h$, and $b = h$ or $b = k$, respectively. (In this paper we use an oblique case of the Lambert azimuthal projection, therefore our k for that projection is in fact k', the scale factor in a direction perpendicular to the radius from the center, see Snyder 1987, 185). For the purposes of our investigations we will use for scale distortion $|k-1|$, which has a value of 0.0 at the points of

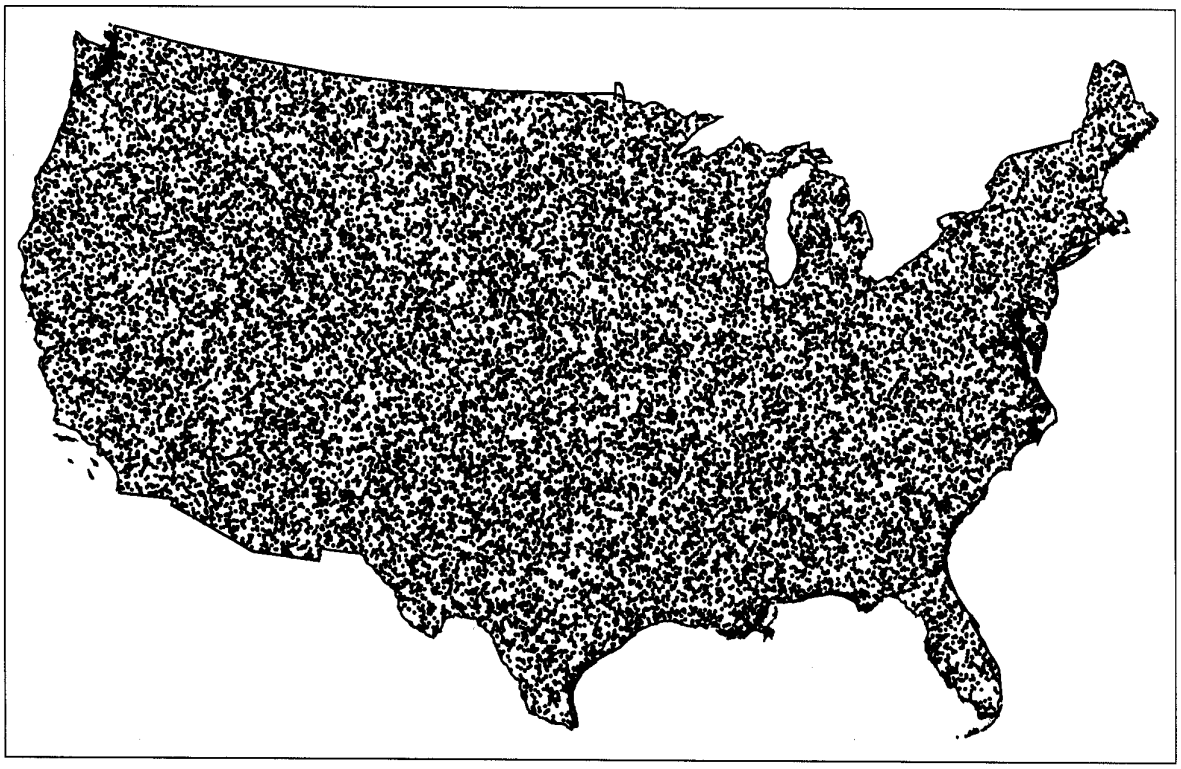

25,000 Unrestricted Random Sample Points

Figure 2. A 25,000-point random sample in the conterminous United States.

development and positive values elsewhere, the same behavior as the other two measures. The geometric relationships between a, b, ω, and z' (the unnormalized z for the general case) are shown in Figure 1.

Statistical Representation

The random variable defined by the chosen measure of shape distortion at a randomly selected point in the study region is completely characterized by its CDF. This function characterizes the proportion of the study region in which distortion is less than a particular value. Quantiles are read directly from the CDF; the median, the 10th percentile, and quartiles are all examples of parameters that are simply read. The mean and standard deviation are also determined by the distribution function, but cannot be determined easily or precisely from the plot. It is common to supplement the plot by reporting a few parameters that have particular interest. The CDF is also known in cartography as a cumulative frequency curve.

Comparison of the sample distribution function to the CDF of known theoretical distributions may also be of interest, although more for the underlying form of distortion patterns than in the integral over the irregular region. Further, certain statistical distributions, like the normal, are of no comparative interest; for the measure we have chosen, distortion is bounded below by zero, whereas the normal is centered at the mean and symmetric to $\pm \infty$. One might compare the distortion distribution to a gamma CDF, but this would be meaningful only if a particular gamma distribution were implied by some feature or hypothesis.

Comparison of two distribution functions is straightforward, particularly in our context where we have a sufficiently large sample size. We can describe differences between projections by reference to particular features of the CDFs, without resorting to statistical tests. It may also be of interest to compare parameters, such as means and standard deviations, and again the issue of statistical significance does not arise. Any difference that might conceivably be considered of practical interest will be statistically significant. We demonstrate this in the analysis section below. This statistical description, coupled with traditional distortion isoline maps, gives a very clear picture

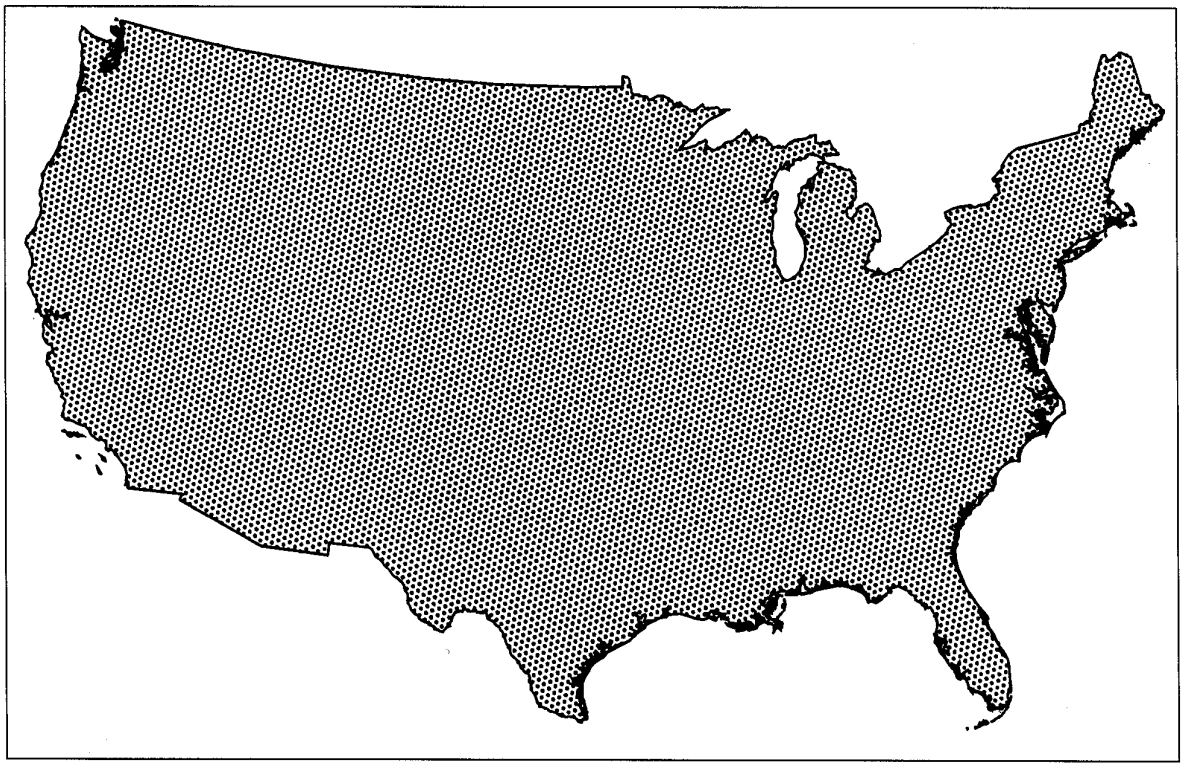

Figure 3. An 11,995-point systematic sample in the conterminous United States obtained from an equilateral triangular grid.

of the geographic distribution of distortion over an irregular area, such as the conterminous United States, or some portion thereof.

Distortion Analysis Experiments

Sample Points

We created a set of 25,000 randomly positioned sample points within the conterminous United States. We created this set by generating over 50,000 pairs of random numbers, which were scaled to the coordinate space of a cylindrical equal area projection of a bounding quadrilateral for the United States (25°-50°N, 65°-125°W). We then clipped these points to the boundary of the conterminous United States. An unrestricted (independent) random sample of 25,000 points found by this protocol formed the sample (Figure 2). Finally we converted each point from map projection to geographic (latitude, longitude) coordinates using the inverse cylindrical equal area projection equations for the sphere.

We obtained systematic sample points from the equilateral triangular point sample (with approximately 27-km spacing between points) described in White et al. (1992). We also clipped these to the United States boundary, obtaining 11,995 points (Figure 3). For the purpose of comparing the random and systematic samples, we also used the first 11,995 points of the random sample.

For subsets in New England and Nebraska we clipped the random and systematic samples to the boundaries of these areas. New England is defined as the states of Maine, New Hampshire, Vermont, Massachusetts, Rhode Island, and Connecticut.

Analysis

We conducted a series of experiments. First we analyzed the distortion functions of the two projections on that portion of their domains sufficient to cover the conterminous United States. This reveals the behavior of these functions along transects of maximum variation. Then we did three sets of sampling experiments. These comprise three geographical domains, two different sampling designs, and six statistics for each of

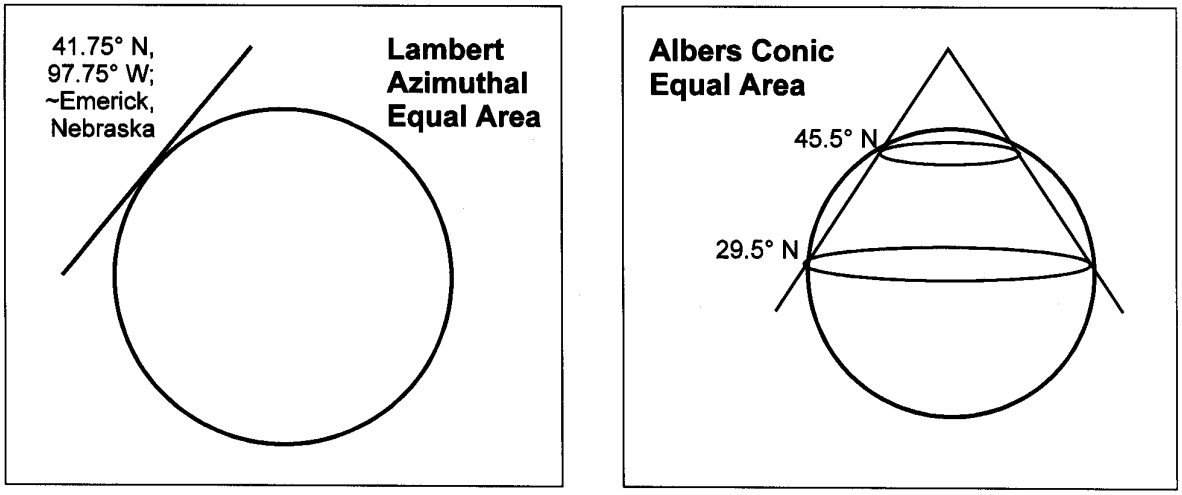

Figure 4. The geometry of the Lambert azimuthal equal area projection (left) and the Albers conic equal area projection (right) positioned for this study.

three different distortion measures for the two projections. For the conterminous U.S. we also varied the sample size for one of the designs. The experiments are summarized in Table 1. In the following discussion we highlight some of the results. The complete results are listed in Appendix 2.

Geographical domains:	conterminous United States, New England, Nebraska
Sampling designs:	random, systematic
Distortion measures:	$\|k - 1\|$, ω, z
Statistics:	minimum, maximum, median, mean, standard deviation, CDF
Map projections:	Lambert, Albers

Table 1. Parameters investigated in sampling experiments.

In our analysis, we used the Lambert azimuthal equal area projection centered at 41°45′N, 97°45′W (in northeastern Nebraska). We selected this center position by visual inspection to cover the area of interest as described in White et al. (1992). We used the standard parameters for the Albers conic equal area projection as it is positioned for the conterminous United States with standard parallels at 29°30′N and 45°30′N (Figure 4).

First, we describe the distortion patterns of the two projections across the steepest gradients of distortion values. For the Lambert projection, this gradient is along a radius from the projection center and, for the Albers, it is along a meridian. In Figure 5 we graph the three distortion measures for the Lambert projection as a function of the angle of arc from the center of the projection. We computed the Lambert distortion measures for each 0.1 degree of arc for 26 degrees from the center, a distance sufficient to cover the conterminous United States from our selected center. In Figure 6 we graph the same distortion measures for the Albers projection distortion as a function of latitude. We computed the Albers distortion measures for each 0.05 degree of latitude between latitudes 24 and 50, spanning the area of interest.

All distortion functions for the Lambert projection increase with distance from the center. The Albers distortion functions, however, show bimodal minima at the standard parallels with a local maximum between them. Note that the Albers functions are only approximately, not precisely, symmetric about a midpoint. Distortion functions of a secant cylindrical projection could be expected to be symmetric. For both projections, the shape distortion functions increase less sharply than the scale or angular distortion functions, but exhibit the same qualitative behavior.

In Figures 7 and 8 we show the CDFs for each distortion measure for the Lambert and Albers projections, respectively. The Lambert CDFs display the smooth cumulative behavior that would be expected from the shape of the distortion functions in Figure 5. The Albers CDFs, however, have a sharp break at a sample proportion of about 0.9. These breaks occur at distortion values equal to the local maxima between the standard parallels and help to describe the optimal distortion performance in the area

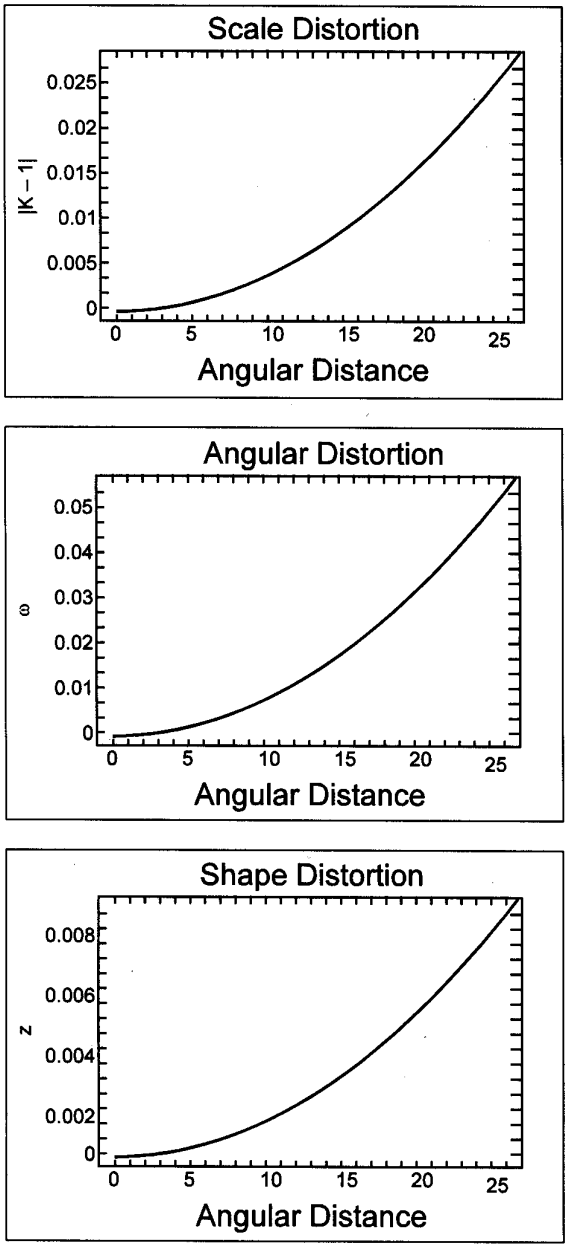

Lambert Projection Distortion Functions by Angular Distance from Center

Figure 5. Scale, angular, and shape distortion functions of the Lambert projection.

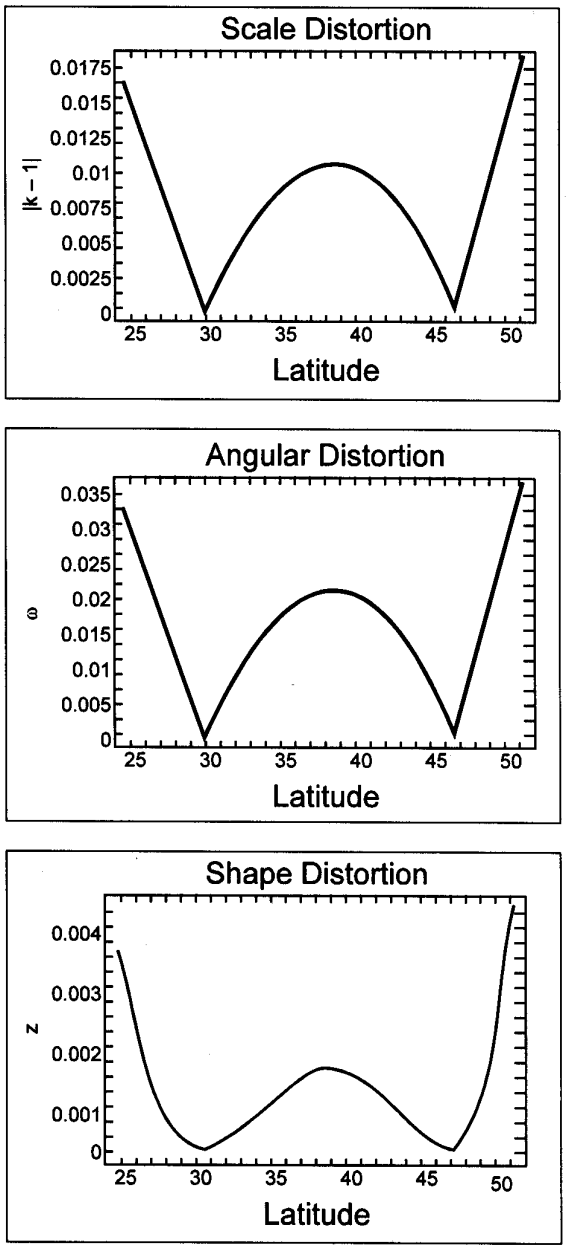

Albers Projection Distortion Functions Across Latitude Transect

Figure 6. Scale, angular, and shape distortion functions of the Albers projection.

immediately surrounding and between the standard parallels, and the marked increase in distortion in latitudes north and south of this optimal area. This behavior in the Albers CDFs is also apparent in our samples over the entire conterminous U.S. (see Figures 11 and 12).

We then computed the distortion measures over the conterminous U.S. Figures 9 and 10 graph the distortion statistics for the 25,000-point URS for both projections for scale and shape distortion, respectively. (Since scale and angular distortion behave nearly identically, we omit discussion of angular distortion henceforward.) The results reveal a significant difference in distortion behavior between the two projections: while the Albers projection has lower maximum distortion

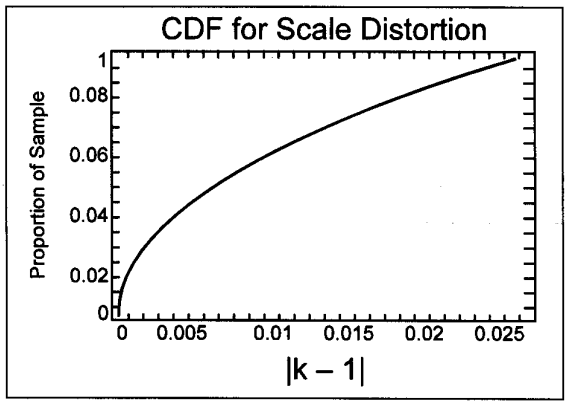

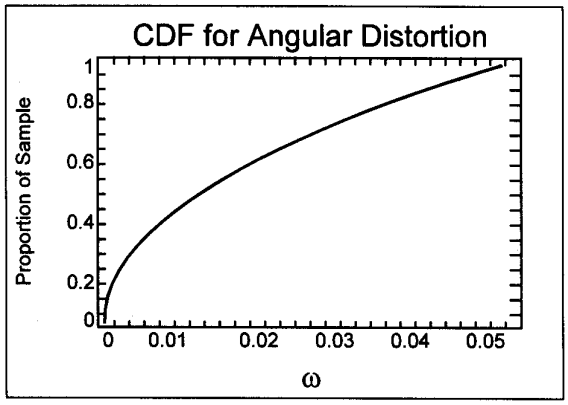

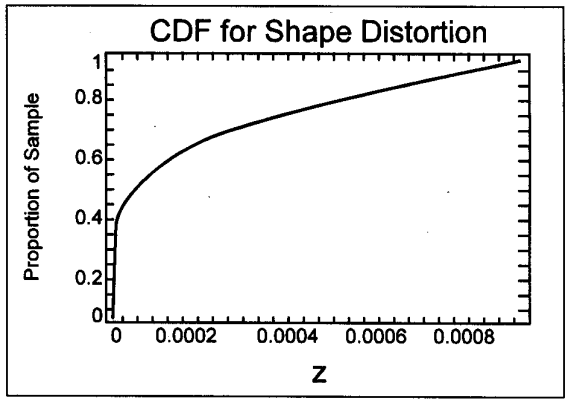

CDFs for Distortion Functions of the Lambert Projection

Figure 7. CDFs for the Lambert distortion functions.

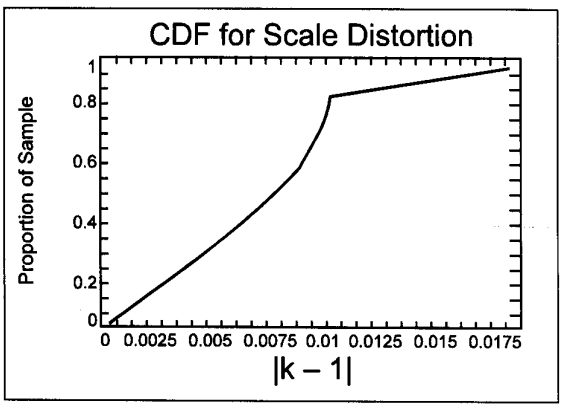

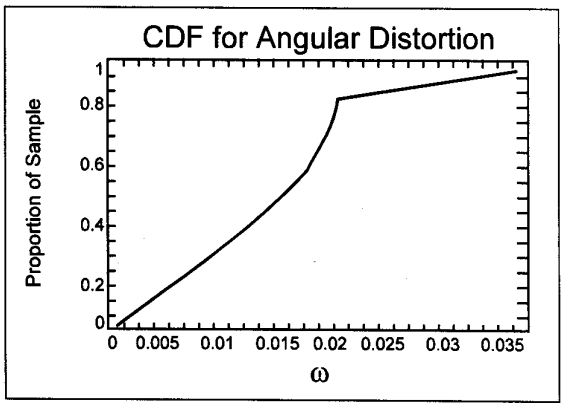

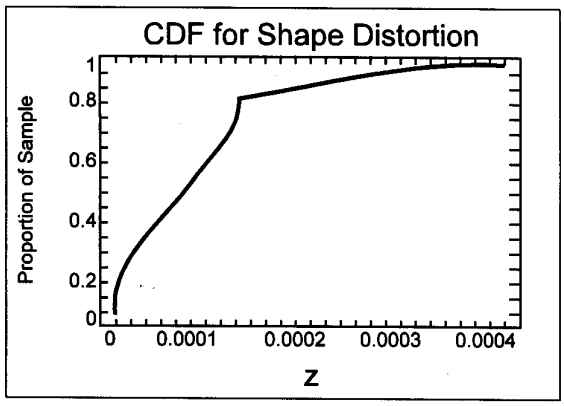

CDFs for Distortion Functions of the Albers Projection

Figure 8. CDFs for the Albers distortion functions.

values and lower variances, the Lambert has lower means and medians. This suggests that for some purposes, such as minimizing mean distortion, the Lambert performs better (even though it may not be optimally centered for this purpose).

In Figures 11 and 12 we show the sample CDFs for scale and shape distortion, respectively. On these graphs we show both the Lambert and Albers graphs simultaneously since they are both derived from the same sample and thus we can compare them directly. For both distortion measures the Lambert projection has lower distortion values over about 80% of the sample points. This demonstrates how the CDF, in addition to the statistics of central tendency and dispersion, is another important statistic for comparing projection performance, and how in this case the Lambert performs better than the Albers over a large portion of the area of interest.

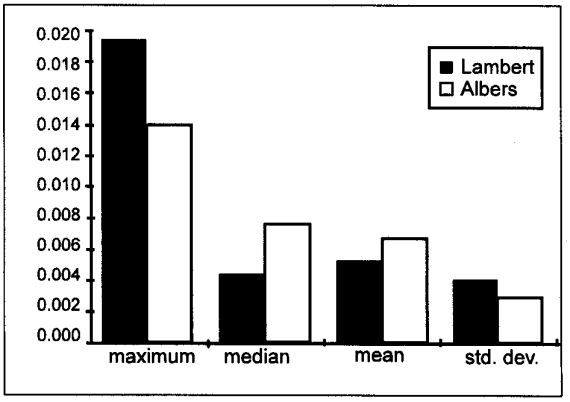

Scale Distortion Statistics for the 25,000-Point Random Sample over the U.S.

Figure 9. Scale distortion statistics for the 25,000-point random sample over the conterminous United States.

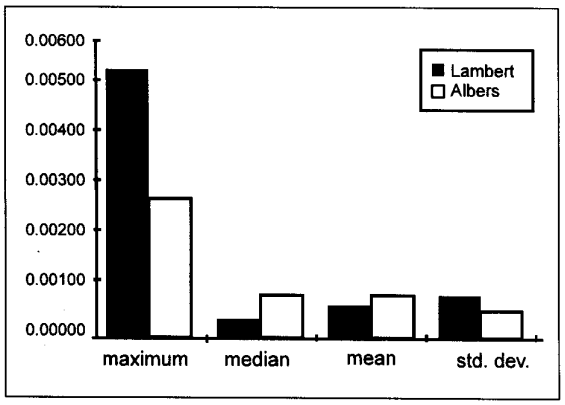

Shape Distortion Statistics for the 25,000-Point Random Sample over the U.S.

Figure 10. Shape distortion statistics for the 25,000-point random sample over the conterminous United States.

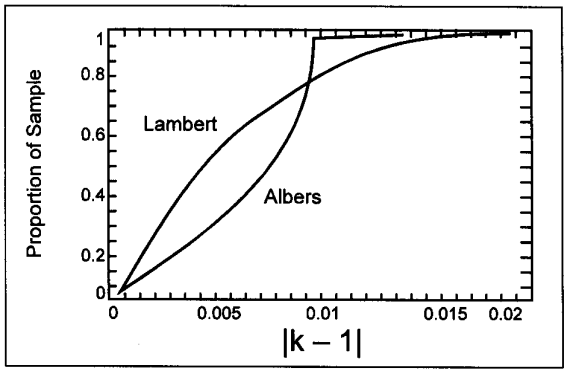

CDFs for Scale Distortion on the 25,000-Point Random Sample over the U.S.

Figure 11. Sample CDFs for both Lambert and Albers scale distortion on the 25,000-point random sample over the conterminous United States.

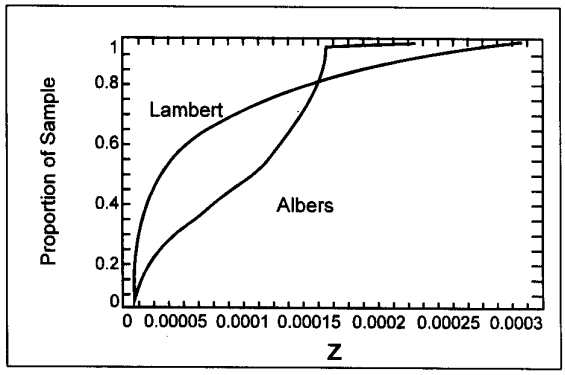

CDFs for Shape Distortion on the 25,000-Point Random Sample over the U.S.

Figure 12. Sample CDFs for both Lambert and Albers shape distortion on the 25,000-point random sample over the conterminous United States.

Random vs. Systematic Sampling

We can analyze the effects of random vs. systematic sampling by holding constant all parameters except the sampling method. For this experiment, we compared the 11,995-point systematic sample with the first 11,995 points of the 25,000-point URS. In Figures 13 and 14 we present the sample CDFs for scale and shape distortion, respectively, for the systematic samples. There is no discernible difference when we overlay these graphs with those in Figures 11 and 12. The CDFs for the 11,995-point random samples are likewise essentially identical and we do not display them here.

These statistics support the contention that random and systematic samples produce virtually indistinguishable results for samples the size of our experiments over the United States. They further support the assertion that the sample size (25,000) used in these analyses is sufficiently large that apparent differences between the distortion measures of the respective projections can be considered real. Maximum distortion is the only statistic for which we do not necessarily obtain a good estimate. There are only a few places in the U.S. where the distortion measures approach their maximum values, and the number of sample points falling in those places will be small. This is the kind of error that one must anticipate in Monte Carlo integration. To determine maximum distortion, one should not take a random sample of points but rather identify it at the points for which it is calculated to be maximum. Therefore, we determined the maximum scale distortion for each projection by calculating the values for each point on the boundary of the conterminous U.S.;

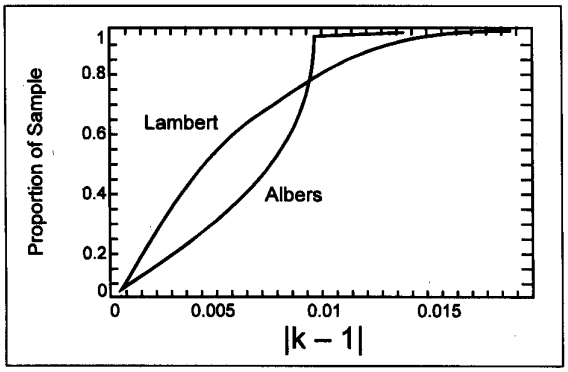

CDFs for Scale Distortion on the 11,995-Point Systematic Sample over the U.S.

Figure 13. Sample CDFs for both Lambert and Albers scale distortion on the 11,995-point systematic sample over the conterminous United States.

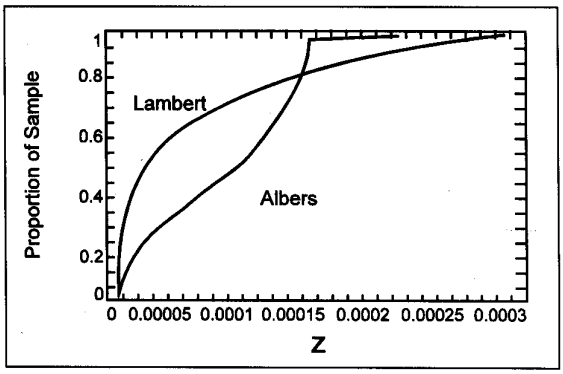

CDFs for Shape Distortion on the 11,995-Point Systematic Sample over the U.S.

Figure 14. Sample CDFs for both Lambert and Albers shape distortion on the 11,995-point systematic sample over the conterminous United States.

the points with maximum value for each projection are shown in Figure 15.

Even though we have demonstrated the virtual identity in performance of the two sampling designs for so large a sample, this does not prove the general properties of the sampling methods but merely provides a confirmatory example. In the case of URS, conventional sampling theory can provide stronger evidence in the form of a basic relation between precision and sample size (n); that is, precision varies as $\sqrt{n}$. From this, we can strongly assert the level of precision of specific descriptive estimates. For example, 95% confidence bounds on the population mean are

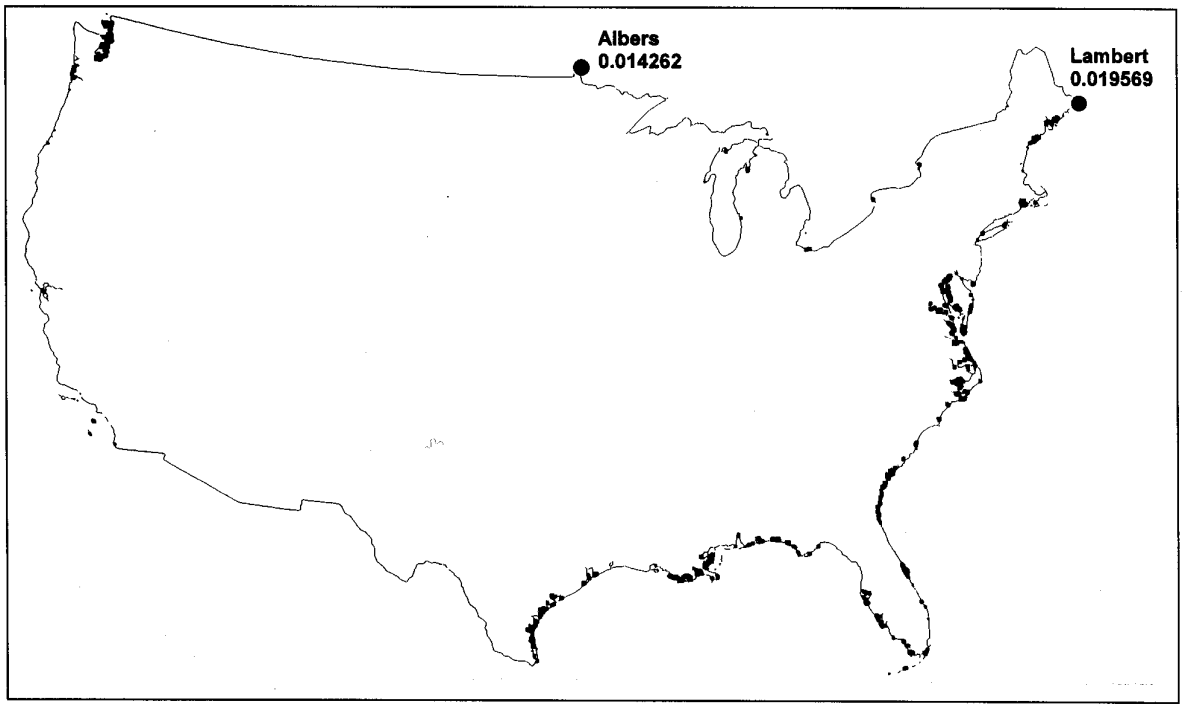

Points of Maximum Scale Distortion

Figure 15. Points in the conterminous United States with maximum scale distortion values for the Lambert and Albers projections.

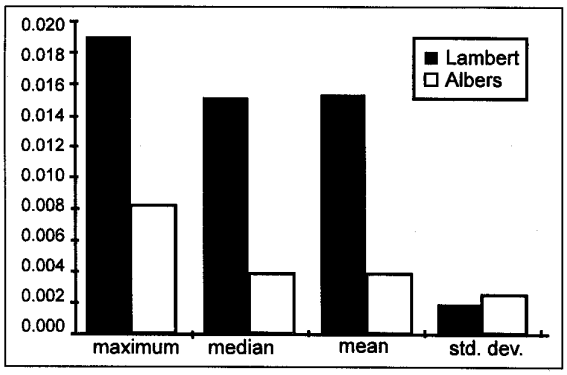

Scale Distortion Statistics for the 263-Point Systematic Sample over New England

Figure 16. Scale distortion statistics for the 263-point systematic sample over New England.

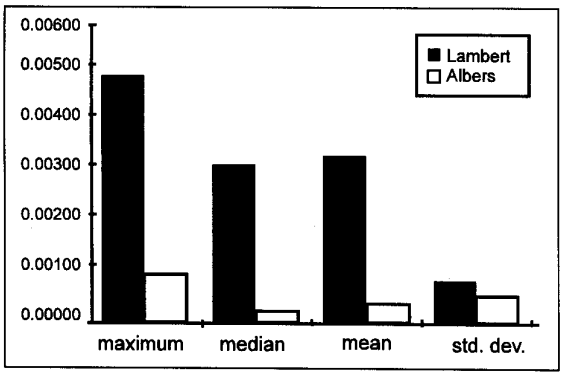

Shape Distortion Statistics for the 263-Point Systematic Sample over New England

Figure 17. Shape distortion statistics for the 263-point systematic sample over New England.

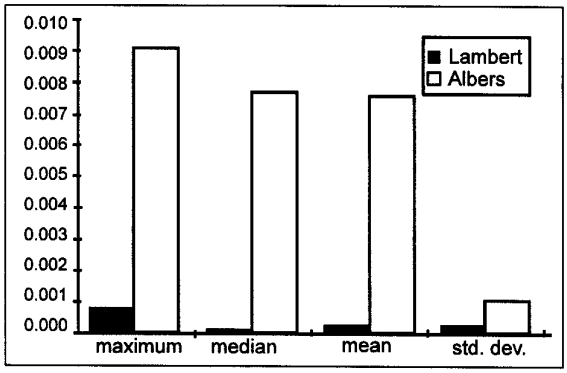

Scale Distortion Statistics for the 307-Point Systematic Sample over Nebraska

Figure 18. Scale distortion statistics for the 307-point systematic sample over Nebraska.

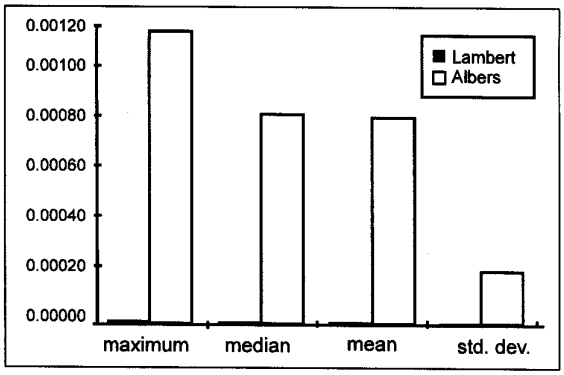

Shape Distortion Statistics for the 307-Point Systematic Sample over Nebraska

Figure 19. Shape distortion statistics for the 307-point systematic sample over Nebraska.

given by $\frac{1.96\,s}{\sqrt{n}}$, where s is the sample standard deviation as reported in Appendix 2.

For example, we compute the half width of the confidence bound on the true mean shape distortion over the United States, for the Lambert projection and our URS of 25,000 points, to be $0.1008 \cdot 10^{-5}$, which is about 1.6% of the estimated mean distortion of $0.624 \cdot 10^{-4}$. Expressed in another way, we are confident that the true mean is between $0.614 \cdot 10^{-4}$ and $0.634 \cdot 10^{-4}$. Similarly, we are confident from the URS of size 11,995 that the true mean shape distortion is between $0.610 \cdot 10^{-4}$ and $0.639 \cdot 10^{-4}$, based on a half width of $0.1455 \cdot 10^{-5}$. Analysis for the Albers shape distortion on the 25,000-point URS gives a confidence bound half width of $0.6010 \cdot 10^{-6}$, with corresponding confidence bounds between $0.743 \cdot 10^{-4}$ and $0.755 \cdot 10^{-4}$.

Earlier, we contended that an estimate close enough to require a test of significance would be of no interest. We have taken this position because there is very little cost involved in taking additional observations, so that we can determine the minimum sample size required for a desired accuracy and then make the sample considerably larger than that.

There is no theoretical basis on which to make similar statistical assessments for the systematic design. Reasonable confidence bounds can be generated, but the calculations cannot be extended to larger or smaller samples on a theoretical basis. Furthermore, the statistics provided here are inadequate to produce confidence bounds. On the other hand, the appropriate confidence bound half width for the systematic sample will be bounded above by that computed for the URS, so the URS analysis can serve as a crude planning tool.

We note that the context of this application is different from many examples of statistical analysis because some traditional sampling concepts are no

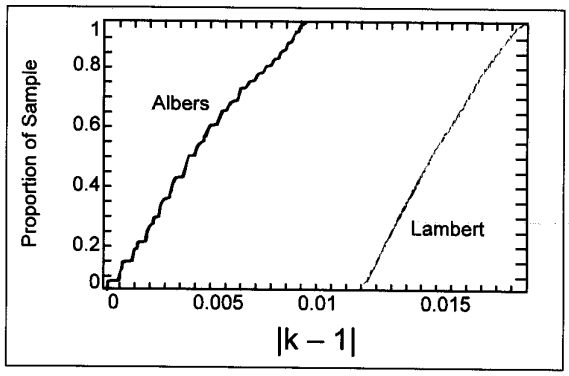

CDFs for Scale Distortion on the 263-Point Systematic Sample over New England

Figure 20. Sample CDFs for both Lambert and Albers scale distortion on the 263-point systematic sample over New England.

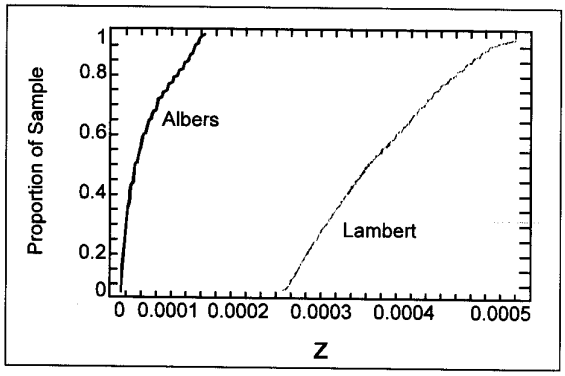

CDFs for Shape Distortion on the 263-Point Systematic Sample over New England

Figure 21. Sample CDFs for both Lambert and Albers shape distortion on the 263-point systematic sample over New England.

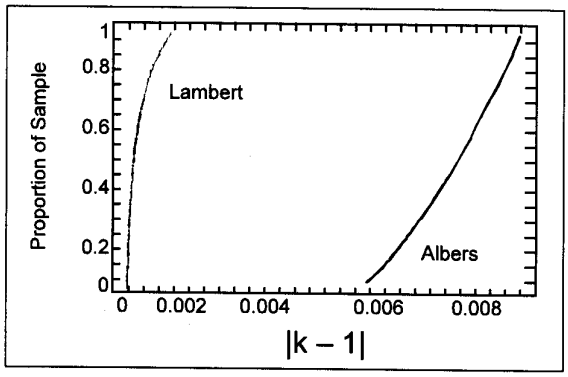

CDFs for Scale Distortion on the 307-Point Systematic Sample over Nebraska

Figure 22. Sample CDFs for both Lambert and Albers scale distortion on the 307-point systematic sample over Nebraska.

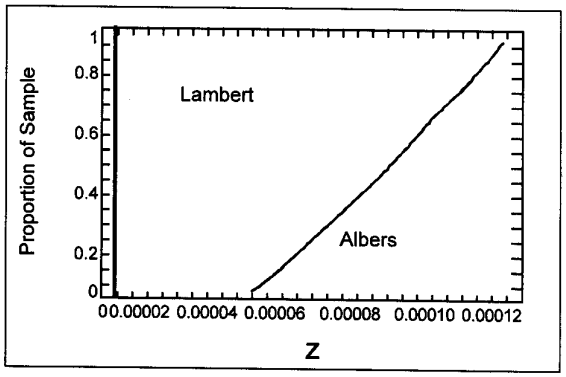

CDFs for Shape Distortion on the 307-Point Systematic Sample over Nebraska

Figure 23. Sample CDFs for both Lambert and Albers shape distortion on the 307-point systematic sample over Nebraska.

longer relevant, for example, sampling efficiency. A reasonable strategy for sampling the distortion measures is to estimate an adequate sample size and then double or triple it. There is little virtue in parsimony in this context because additional observations can be obtained at almost no cost. In contrast, a field sample will require a substantial investment in collecting and processing each datum, so that efficient sampling is imperative.

Subpopulations

One great advantage of the sampling approach to numerical integration, as we illustrate here, is a straightforward application to an analysis of any identified subpopulation. The process consists of simply identifying any subset of the region occupied by the population in such a manner that sample points can be classified as in or as not in this subset. The subset of the sample can then be used to generate the distributional characteristics of the subpopulation, as we now illustrate with two simple cases. The state of Nebraska and the New England region provide two such subpopulations. The subset of a URS contained in any such region is a conditional URS for that region. Similarly, for a randomized systematic sample, the portion contained in any subregion is a randomized systematic sample of that subregion. The universality of the method, and the ease of application to a variety of objectives and subpopulations, make the method doubly attractive.

In Figures 16 and 17 we graph the scale and shape distortion statistics, respectively, for the systematic sample of New England. Since one of the standard parallels for the Albers projection crosses New England, the distortion for this

projection is low; in contrast New England is at a great distance from the center of the Lambert projection and therefore the Lambert distortion is high. In Figures 18 and 19 we show the scale and shape distortion statistics, respectively, for the Nebraska systematic sample where the situation is reversed. In Figures 20, 21, 22, and 23 we show the CDFs that correspond to the graphs in Figures 16, 17, 18, and 19. The contrast between the two projections in these two areas is also evident in the CDFs. The full results of these experiments are in Appendix 2.

Conclusion

The statistical analysis of map projection distortion, as indicated by scale, angular, and total shape deformation for equal area projections, demonstrates that the Lambert azimuthal equal area projection is well suited for an irregular area with the shape of the conterminous United States. In particular, the Lambert projection has a smaller mean distortion than the Albers conic equal area, whereas the Albers projection has smaller mean squared distortion, as shown by the smaller standard deviation. Using the latter criterion, we would prefer the Albers projection. On the other hand, we might prefer the Lambert projection since approximately 80% of the conterminous U.S. has lower distortion with it. Our contention is that the statistical approach to map projection distortion comparison makes such distinctions possible.

We have shown statistical sampling of map projection distortion surfaces as a simulation of numerical integration to be satisfactory under both random and systematic sampling designs. Although systematic sampling is somewhat more precise than unrestricted random sampling for any specific sample size, the distinction is unimportant in this context. A simple increase in size of the URS will capture any difference in precision. For the analyses made in this paper, the URS is superior, since the estimator of the population standard deviation is unbiased and the theory of independent random samples can be used to make assessments that cannot be made for the systematic sample. For other analyses—for example, generating a map of the spatial patterns of distortion—a systematic sample would be superior.

Whatever the objective of comparison of projections, the statistical approach to map projection distortion analysis provides a useful tool for understanding and comparing the nature of the distortion or other spatially varying features over specific irregular regions. The URS is better suited to this purpose than the systematic sample of points, although, for samples as large as those used here for the U.S., there is little difference in the results from the two sampling designs.

ACKNOWLEDGMENTS

We would like to acknowledge the assistance of George Weaver in statistical analysis and graphics. This research has been partially supported by EPA contracts 68-C8-0006 with ManTech Environmental Technology, Inc., and 68-C0-0021 with Technical Resources Inc., and by cooperative agreements CR816721 and CR821672 with Oregon State University.

REFERENCES

Dyer, J. A., and J. P. Snyder. 1989. Minimum-error equal-area map projections. *The American Cartographer* 16:39-43.

Hammersley, J. M., and D. C. Handscomb. 1964. *Monte Carlo methods.* Methuen's Monographs on Applied Probability and Statistics. New York: Wiley.

Maling, D. H. 1973. *Coordinate systems and map projections.* London: George Philip.

Maling, D. H. 1989. *Measurements from maps: Principles and methods of cartometry.* Oxford: Pergamon.

Matérn, B. 1986. *Spatial variation.* 2nd edn. Lecture notes in statistics, number 36. Berlin: Springer-Verlag.

Moran, P. A. P. 1950. Numerical integration by systematic sampling. *Proceedings of the Cambridge Philosophical Society* 46:111-15.

Muehrcke, P.C. 1986. *Map use.* 2nd edn. Madison, Wis.: JP Publications.

Press, W. H., B. P. Flannery, S. A. Teukolsky, and W. T. Vetterling. 1988. *Numerical recipes in C.* Cambridge: Cambridge University Press.

Robinson, A. H. 1951. The use of deformational data in evaluating world map projections. *Annals, Association of American Geographers* 41:58-74.

Robinson, A. H., J. L. Morrison, P.C. Muehrcke, A. J. Kimmerling, and S. C. Guptill. 1995. *Elements of cartography.* 6th edn. New York: Wiley.

Snedecor, G. W., and W. G. Cochran. 1980. *Statistical methods.* 7th edn. Ames: Iowa State University Press.

Snyder, J. P. 1987. *Map projections—A working manual.* U.S. Geological Survey professional paper 1395. Washington D.C.: USGPO.

Snyder, J. P. 1994. How practical are minimum-error map projections? *Cartographic Perspectives* 17(4): 3-9

Tobler, W. R. 1964. *Geographical coordinate computations: Part II Finite map projection distortions.* Technical report no. 3. ONR Task No. 389-137. Department of Geography, University of Michigan.

White, D., A. J. Kimerling, and W. S. Overton. 1992. Cartographic and geometric components of a global sampling design for environmental monitoring. *Cartography and Geographic Information Systems* 19(1): 5-22.

Yates, F. 1949. Systematic sampling. *Philosophical transactions of the Royal Society* 241(A): 345-77.

Young, A. E. 1920. *Some investigations in the theory of map projections.* Technical series no. 1. London: Royal Geographical Society. ■

Appendix 1
Distortion Analysis

The following introductory paragraphs are intended to acquaint the reader with the concepts and measures associated with map projection distortion and distortion measures. These underlie the statistical approach to map projection comparison.

Basic to cartography is the fact that a segment of the spherical or spheroidal earth cannot be projected onto a planar surface without introducing some type of geometric distortion. Also well known is that on particular map projections certain geometrical characteristics can be preserved, such as constancy in surface area between globe and map (equivalence), constancy in shape between globe and projection surface in the immediate neighborhood of any point on the projection (conformality), and preservation of angles and distances on the globe outward from the projection center point (equidistance). Projections with equivalence throughout are called equal area, those with conformality everywhere are termed conformal, and those with equidistance are called equidistant. Unfortunately, no single map projection can have all three characteristics, let alone be conformal and equal area simultaneously.

Equivalence, conformality, and equidistance, or lack thereof, are projection properties first described mathematically by Lambert in the eighteenth century, and then further investigated by Gauss and Tissot in the nineteenth century. In the 1820s Gauss employed partial derivatives to determine what are called *particular scales*, meaning "the relation between an infinitesimal linear distance in any direction at any point on a map projection and the corresponding linear distance on the globe" (Maling 1973, page 63). The ratio of these linear distances gives the amount of scale distortion in the particular direction. Of special interest is scale distortion in the directions of the meridian and parallel passing through the point, termed h and k distortion, respectively. Also important is the angle on the map projection, termed θ', formed by the intersection of the parallel and meridian, knowing that all parallels and meridians intersect at 90° angles on the globe.

In the 1850s, Tissot carried forth the work of Gauss in several ways, one of which has become known as Tissot's Theorem: "Whatever the system of projection there are at every point on one of the surfaces two directions perpendicular to one another and, if angles are not preserved, there are only two of them [perpendicular directions], such that the directions which correspond to them on the other surface also intersect one another at right angles" (Maling 1973). These orthogonal directions are termed the *principal directions* at a point.

Tissot's well-known indicatrix next comes into play. The idea behind the indicatrix is that "an infinitely small circle on the surface of the globe will be transformed on the plane into an infinitely small ellipse whose semi-axes lie along the two principal directions" (Maling 1973). The lengths, a and b, of the semi-major and semi-minor axes of the ellipse indicate the maximum scale enlargement and reduction at the point on the projection relative to the globe. The amount of area distortion is given by the product $a \cdot b$, which Gauss determined to be equal to $h \cdot k \cdot \sin \theta'$. On equal area projections, $a \cdot b = 1.0$, whereas $a = b$ on conformal and a or $b = 1.0$ on equidistant projections.

On many azimuthal, conic, and cylindrical projections (in normal aspect), $\theta' = 90°$, so that $h \cdot k = a \cdot b$. Hence, for the equal area versions of these three projection types, $h \cdot k = 1.0$, so that $h = 1/k$. Another measure related to scale distortion is the maximum angular deformation, ω, which indicates the maximum deflection of any azimuth at a point on the globe when projected. The equation, $\omega = 2 \cdot \sin^{-1}[(a-b)/(a+b)]$, is used commonly to find the maximum angular deformation at any point on the projection.

Appendix 2
Results of Experiments

	U.S. 25,000-point random sample	U.S. 11,995-point random sample	U.S. 11,995-point systematic sample
Lambert $\lvert k - 1 \rvert$			
minimum	0.000000105656	0.000002181248	0.000000026782
maximum	0.019518537294	0.019518537294	0.019145526405
median	0.004449347683	0.004431322894	0.004471964345
mean	0.005320085497	0.005319218037	0.005351944406
std. dev.	0.004034861724	0.004039316482	0.004079002611
Lambert ω			
minimum	0.000000211312	0.000004362491	0.000000053565
maximum	0.038658579692	0.038658579692	0.037926840647
median	0.008878928032	0.008843038170	0.008923960035
mean	0.010595741805	0.010593980987	0.010658766128
std. dev.	0.008014573583	0.008023467706	0.008101839051
Lambert *z*			
minimum	0.000000000000	0.000000000007	0.000000000000
maximum	0.000528413434	0.000528413434	0.000508597687
median	0.000027872601	0.000027647726	0.000028156047
mean	0.000062403611	0.000062439864	0.000063373471
std. dev.	0.000081309105	0.000081307732	0.000082793152
Albers $\lvert k - 1 \rvert$			
minimum	0.000000774930	0.000002081176	0.000005360482
maximum	0.014170927748	0.014170927748	0.013388290878
median	0.007469524690	0.007500013734	0.007470314812
mean	0.006647787048	0.006659865854	0.006629512688
std. dev.	0.002905175262	0.002910419016	0.002921134452
Albers ω			
minimum	0.000001549861	0.000004162356	0.000010720992
maximum	0.028141988825	0.028141988825	0.026598135314
median	0.014991803417	0.015054474446	0.014987862557
mean	0.013336325720	0.013360523201	0.013299580914
std. dev.	0.005834789611	0.005845036834	0.005866892723
Albers *z*			
minimum	0.000000000001	0.000000000006	0.000000000041
maximum	0.000280013464	0.000280013464	0.000250132540
median	0.000079463343	0.000080129108	0.000079421571
mean	0.000074919253	0.000075189444	0.000074705500
std. dev.	0.000048481768	0.000048706235	0.000048659742

	New England 1,166-point random sample	New England 263-point systematic sample	Nebraska 1,402 -point random sample	Nebraska 307-point systematic sample
Lambert $\|k - 1\|$				
minimum	0.012420714839	0.012363590439	0.000000105656	0.000000026782
maximum	0.019518537294	0.019145526405	0.000865845106	0.000853359897
median	0.015126128433	0.015210325420	0.000139462271	0.000134937983
mean	0.015333822728	0.015377209726	0.000219354466	0.000221059109
std. dev.	0.001808530342	0.001804960020	0.000214439383	0.000220340705
Lambert ω				
minimum	0.024687794223	0.024574952441	0.000000211312	0.000000053565
maximum	0.038658579692	0.037926840647	0.001730940741	0.001705991778
median	0.030024610644	0.030190469750	0.000278905093	0.000269857759
mean	0.030430503592	0.030515977571	0.000438614882	0.000442020977
std. dev.	0.003561334705	0.003554254596	0.000428728588	0.000440526833
Lambert *z*				
minimum	0.000215491734	0.000213526268	0.000000000000	0.000000000000
maximum	0.000528413434	0.000508597687	0.000001059301	0.000001028985
median	0.000318732313	0.000322263593	0.000000027502	0.000000025747
mean	0.000331889942	0.000333700911	0.000000132957	0.000000137467
std. dev.	0.000077700815	0.000077617362	0.000000222741	0.000000229202
Albers $\|k - 1\|$				
minimum	0.000011551382	0.000030821077	0.005569818468	0.005580511348
maximum	0.008123329343	0.008021655312	0.009071795671	0.009068814790
median	0.003449399555	0.003528361366	0.007746334766	0.007674313855
mean	0.003696526486	0.003710334579	0.007608117079	0.007572308990
std. dev.	0.002267272702	0.002265338671	0.000974445404	0.000975846273
Albers ω				
minimum	0.000023102630	0.000061641205	0.011170717410	0.011192222732
maximum	0.016312825843	0.016107829630	0.018226137674	0.018220121592
median	0.006910711151	0.007069186709	0.015552830172	0.015407673461
mean	0.007408276369	0.007435569885	0.015275220381	0.015203058852
std. dev.	0.004552141643	0.004548018939	0.001963465081	0.001966271152
Albers *z*				
minimum	0.000000000189	0.000000001343	0.000044118364	0.000044288397
maximum	0.000094084530	0.000091734724	0.000117449267	0.000117371744
median	0.000016885017	0.000017668302	0.000085522078	0.000083933133
mean	0.000026724130	0.000026832583	0.000083858371	0.000083081183
std. dev.	0.000026651695	0.000026700323	0.000020805588	0.000020812505